Microstructured Hydrogel Templates for the Formation of Conductive Gold Nanowire Arrays

Wuennemann, Patrick; Noyong, Michael; Kreuels, Klaus; Bruex, Roland; Gordiichuk, Pavlo; van Rijn, Patrick; Plamper, Felix A.; Simon, Ulrich; Boeker, Alexander

Published in:
Macromolecular Rapid Communications

DOI:
10.1002/marc.201600287

Publication date:
2016

Microstructured Hydrogel Templates for the Formation of Conductive Gold Nanowire Arrays

Patrick Wünnemann, Michael Noyong, Klaus Kreuels, Roland Brüx, Pavlo Gordiichuk, Patrick van Rijn, Felix A. Plamper, Ulrich Simon, Alexander Böker*

Microstructured hydrogel allows for a new template-guided method to obtain conductive nanowire arrays on a large scale. To generate the template, an imprinting process is used in order to synthesize the hydrogel directly into the grooves of wrinkled polydimethylsiloxane (PDMS). The resulting poly(N-vinylimidazole)-based hydrogel is defined by the PDMS stamp in pattern and size. Subsequently, tetrachloroaurate(III) ions from aqueous solution are coordinated within the humps of the N-vinylimidazole-containing polymer template and reduced by air plasma. After reduction and development of the gold, to achieve conductive wires, the extension perpendicular to the long axis (width) of the gold strings is considerably reduced compared to the dimension of the parental hydrogel wrinkles (from ≈1 μm down to 200–300 nm). At the same time, the wire-to-wire distance and the overall length of the wires is preserved. The PDMS templates and hydrogel structures are analyzed with scanning force microscopy (SFM) and the gold structures via scanning electron microscopy (SEM) and energy-dispersive X-ray spectroscopy. The conductivity measurements of the gold nanowires are performed in situ in the SEM, showing highly conductive gold leads. Hence, this method can be regarded as a facile nonlithographic top-down approach from micrometer-sized structures to nanometer-sized features.

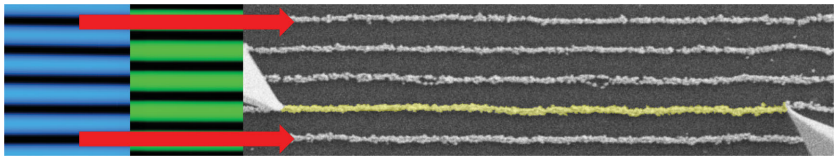

P. Wünnemann, K. Kreuels, R. Brüx
Lehrstuhl für Makromolekulare Materialien und Oberflächen
RWTH Aachen University
Forckenbeckstraße 50, 52056 Aachen, Germany
Dr. M. Noyong, Prof. U. Simon
Institute of Inorganic Chemistry
RWTH Aachen University
JARA-FIT, Landoltweg 1, 52074 Aachen, Germany
P. Gordiichuk, Dr. P. van Rijn
Zernike Institute for Advanced Materials
University of Groningen
A. Deusinglaan 1, 9747AG Groningen, The Netherlands
Dr. P. van Rijn
University Medical Center Groningen
Department of Biomedical Engineering-FB40
University of Groningen
A. Deusinglaan 1, 9713 AV Groningen, The Netherlands
Dr. P. van Rijn
W. J. Kolff Institute for Biomedical Engineering
and Materials Science-FB41
University of Groningen
A. Deusinglaan 1, 9713AW Groningen, The Netherlands
Dr. F. A. Plamper
Institute of Physical Chemistry
RWTH Aachen University
Landoltweg 2, 52074 Aachen, Germany
Prof. A. Böker
Fraunhofer Institute for Applied Polymer Research (IAP) &
Lehrstuhl für Polymermaterialien und Polymertechnologien
University of Potsdam
Geiselbergstraße 69, 14476 Potsdam-Golm, Germany
E-mail: alexander.boeker@iap.fraunhofer.de

DOI: 10.1002/marc.201600287

1. Introduction

The fabrication of uniform conductive gold micro- and nanowires on a large scale is still a challenge. They are of high interest, e.g., in the fields of optoelectronics[1,2] or sensors.[3,4] To meet the need in surface functionalization, many approaches have been developed to produce 1D structures on the micro- and nanoscale, utilizing techniques which can be classified into lithography techniques[5–8] (top-down) and self-assembly processes[9–11] (bottom-up), respectively. In case of top-down processes, electron beam lithography (EBL) techniques are capable of generating defined nanostructures. However as a serial technique with high instrumental effort, EBL are not suitable for large scale productions. In bottom-up approaches, templates are essential to guide uniform 1D micro- and nanostructure generation on a large scale.[12] Most of these processes require prepared metallic nanostructures before deposition.[10,11] Another large-scale approach is nanoskiving.[13,14] By utilizing e-beam and microtome technology, the section procedure requires a skilled user to generate the metallic patterns with a minimum presence of defects.

Here, we present a highly flexible and cost-effective hybrid method, combining the advantages of the top-down guidance with a bottom-up assembly, to fabricate uniform metal nanowire arrays in a two-step process on a large area. Firstly, a microstructured hydrogel film is obtained from a polymerization solution via soft imprint lithography using a wrinkled polydimethylsiloxane (PDMS) stamp with various dimensions as a template. Secondly, the hydrogel structure is used to assemble gold ions in the desired nanostructure before further processing toward gold nanowires (Scheme 1).

To achieve the formation of a microstructured hydrogel for the incorporation of gold ions (the first step), we use PDMS as a well-known foundation to obtain various micro- and nanopatterns in lithography,[15–17] and self-organization processes.[18–20] Oxygen plasma treatment in the stretched state of the PDMS elastomer is a fast and low-cost approach for obtaining microstructured surfaces on a large scale. Hereby, the wrinkled surface is formed spontaneously upon release of strain due to a mismatch in expansion between two layers with different elastic modulus (plasma-oxidized surface of the PDMS specimen vs unaltered bulk PDMS).[18,19] Next to the formation of such microstructured surfaces, many ways have been shown to use wrinkled PDMS as a tool for the alignment of particles for hard[21] and soft matter.[22] In our case, the direct transfer of the PDMS micropatterns to the responsive structure takes place by an imprinting step at room-temperature. Just by pressing the PDMS template on a flat silicon surface modified with a polymerizable functionality, a monomer/crosslinker/initiator mixture is forced into the grooves of the PDMS-wrinkles. The shape of the resulting microstructured hydrogel films, covalently attached to the silicon surface, corresponds to the utilized wrinkled PDMS pattern after polymerization and drying. It defines the later obtained gold nanostructures surface after incorporation and coordination of the applied gold ions during the second step (absorption step). By choosing the appropriate monomer in the hydrogel imprinting process, functional groups allow further modifications. For the purpose of generating a template for gold nanowires, the hydrogel is based on N-vinylimidazole, as it is known to complex metallates like aurates electrostatically (/coordinatively).[23–25] To reduce the coordinated ions, cold plasma is introduced to reduce the gold ions and simultaneously remove the supporting hydrogel.[26]

2. Results and Discussion

The functionalization of the PDMS wrinkles with trichloro(1H,1H,2H,2H-perfluorooctyl)silane was chosen to enhance the hydrophobic behavior and prevent adhesion between the oxidized PDMS surface and the hydrogel. For a covalent binding of the hydrogel on the surface of the silicon substrates, the wafer was also functionalized with 3-(trimethoxysilyl)propylmethacrylate. The available surface bound methacrylate group polymerizes into the chosen hydrogel via radical polymerization which was performed under inert atmosphere (details provided in the Experimental Section). Nitrogen-based polybases such as N-vinylimidazole have the ability to coordinate noble metal ions such as Au(III), for this we chose N-vinylimidazole as the responsive platform for the gold nanowires.[27] The generated structures in the polymerized hydrogel and of the PDMS stamp were compared by means of scanning force microscopy (SFM) (Figure 1).

The upper SFM images in Figure 1 display uniform anisotropic

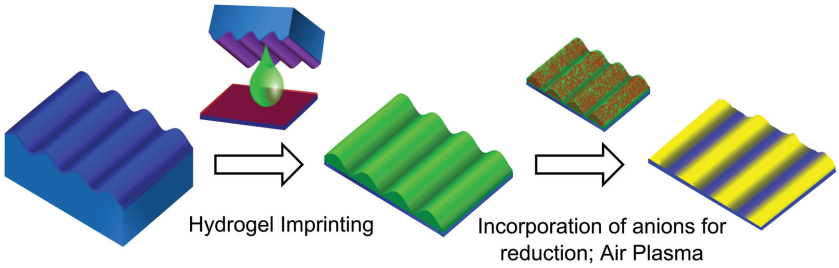

Scheme 1. Fabrication process of wrinkled responsive nanostructures: first, the transfer from wrinkled PDMS to a responsive hydrogel nanopattern via hydrogel imprinting; second, the incorporation and reduction of gold ions in the responsive network as well as the removal of the gel to gain Au nanowire arrays.

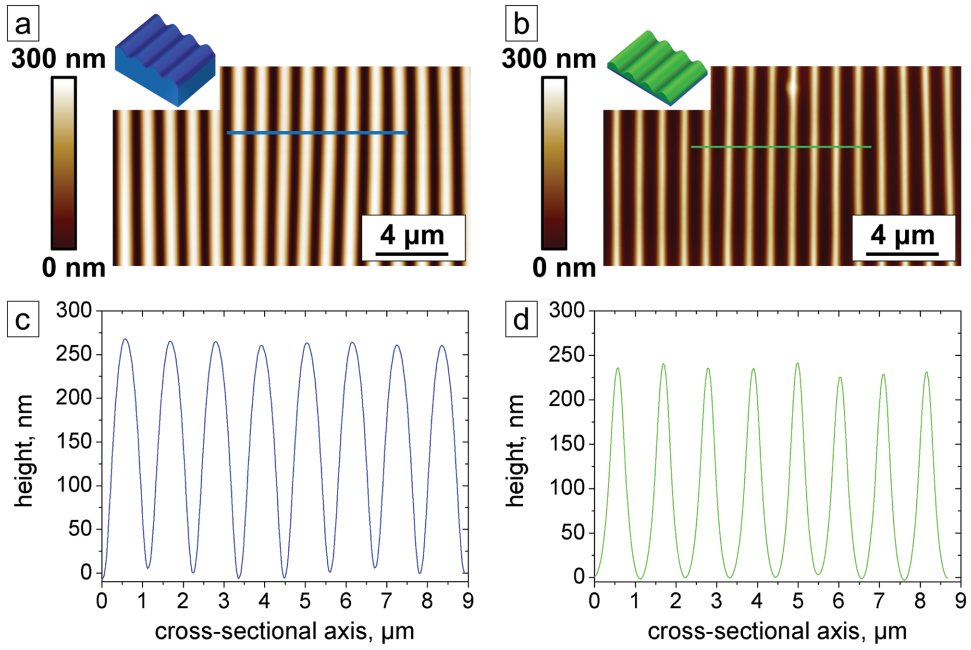

Figure 1. SFM images of nanopattern structures: a) the nonfunctionalized PDMS nanostructure and b) responsive hydrogel nanostructure after the hydrogel imprinting. Bottom: Respective cross-sections of the sinusoidal structure: c) the sinusoidal structure of the PDMS stamp ($A = 262 \pm 6$ nm; $\lambda = 1115 \pm 11$ nm); d) the hydrogel nanopattern imprint ($A = 230 \pm 6$ nm; $\lambda = 1084 \pm 32$ nm).

microstructures of the unmodified PDMS pattern (left) and the hydrogel negative (right), which can be seen in the respective cross-sections of these sinusoidal patterns below (see also Figure S1, Supporting Information). The PDMS stamp was pressed onto the flat silicon wafer during hydrogel imprinting, hence the dimensions of the resulting hydrogel after polymerization was limited to the dimensions of the grooves given by the wrinkled PDMS stamp (see Figure S2, Supporting Information). Considering the values of the amplitude and wavelength of the hydrogel, it can be seen that there was nearly no loss in the measured geometric parameters. The SFM image and the cross-section underneath exhibit a smooth and uniform periodic hydrogel microstructure. To obtain Au-nanoarrays from the responsive hydrogel micropatterns, the hydrogel pattern was immersed in an aqueous tetrachloroaurate solution, dried and reduced using plasma, as shown in Scheme 1, providing gold nanopatterns as shown in Figure 2.

SFM image of the hydrogel structure in Figure 2a resembles the periodic uniform microstructure, which was taken before the gold reduction via air plasma. By partially removing (scratching) the hydrogel structure with a cannula, see left part of the SFM images Figure 2a, c, it was observed that there was an interconnected polymer layer of about 5 nm thickness (see Figure 2d). The layer was most likely formed due to the functionalization of the silicon substrate. However, this thin polymer layer did not influence the formation of separated gold nanowires. With air plasma, the incorporated metal ions were reduced to elemental gold and the carbon-based polymer network was removed during the process.

It was found that the width of the 1D structures was considerably reduced upon plasma treatment (Figure 2c, d). Outgoing from the hydrogel wrinkle, the width is decreased from about 1 µm to only 200 nm. This observation is probably a result of attractive forces of the developing gold nanoparticles toward the region of highest gold density (central long axis of former hydrogel hump) due to strong interparticular van der Waals interactions. At the same time, the wire-to-wire distances and the overall lengths of the wires were similar to the ones of the hydrogel wrinkles indicating that the reduced size is related to internal structural changes assisted by the etching of the polymeric matrix. The process generated granular gold lines, which can be further developed to fully conductive nanowires (see below). Hence, the described method can be regarded as a facile imprint-lithographic top-down method to produce large array nanowire structures (with nanometer-sized features) from micrometer-sized prestructures.

Figure 2e–g displays the corresponding SEM and energy-dispersive X-ray spectroscopy (EDX) analysis of the separated nanostructures. The SEM confirmed the nanoscaled 1D arrangements (Figure S3, Supporting Information). The EDX spectra showed gold, silicon, carbon, and oxygen (see Figures S5 and S6, Supporting Information). Elemental mapping on a selected area displayed the presence of gold corresponding to the nanostructures (Figure S5, Supporting Information).

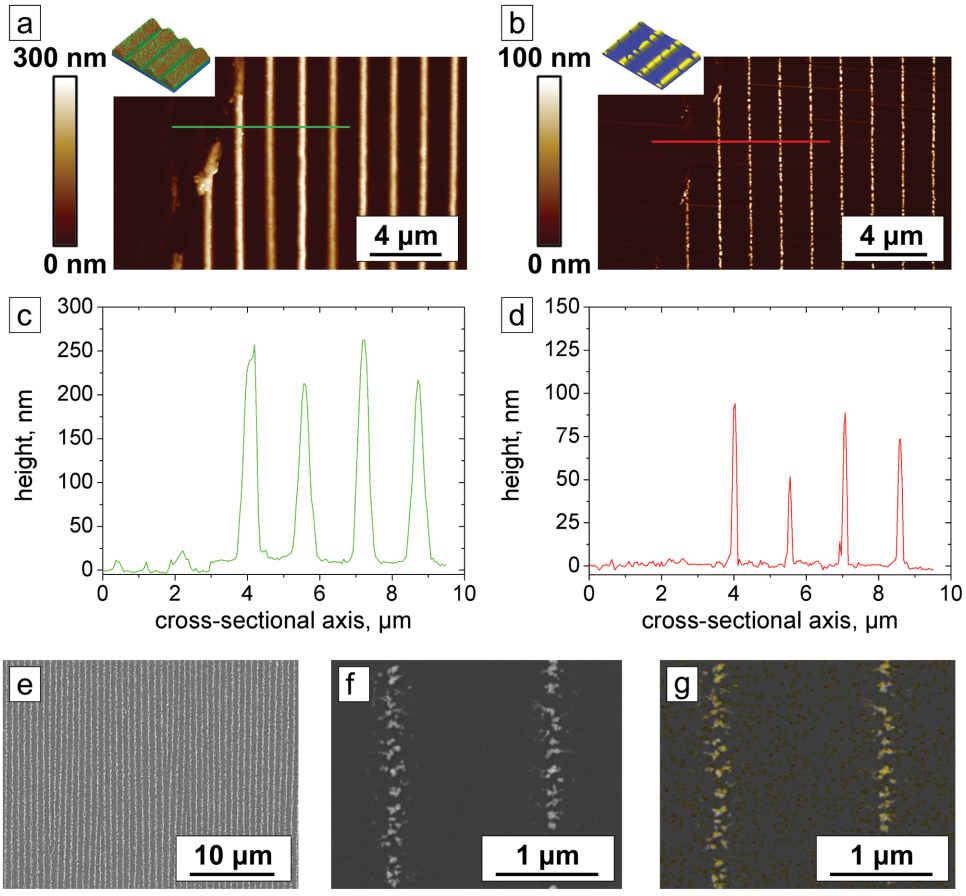

Figure 2. a) SFM image of the hydrogel structure after swelling in aqueous solution with dissolved tetrachloroauric(III) acid and c) its respective cross-section; b) SFM image of the sample after plasma treatment d) with a cross-section; bottom: SEM and EDX images of the Au nanostructure after aurate reduction via air plasma: e) overview of the Au structure, f) magnified area of the structure, and g) EDX of the zoom. Further detailed EDX analysis can be found in Figures S5 and S6 of the Supporting Information.

Upon examining the EDX mapping and overlay image more closely, it was observed that gold is detected on the entire surface. Analyzing the gold nanowire and the areas in between, it became clear that it constitutes as background noise (compare Figure S6, Supporting Information). Further spectra taken on dedicated points of the gold nanostructures and in the gaps in between exemplify the oxidized residues particularly of the functionalization. To connect the aligned but separated gold islands and to generate conductive 1D structures, the gold was successively developed by repeated reduction of an Au(III)-precursor to metallic gold via hydroquinone chemistry (Figure S4, Supporting Information).

Local probe measurements were carried out by in situ conductivity experiments at the SEM to prove conductivity.[28] Individual nanowires were analyzed with different tip–tip distances to investigate the distance dependent conductivity in situ. The tips acting as the electrodes were placed onto a single nanowire structure and conductivity was measured at different tip-to-tip distances. For each tip-to-tip distance, a SEM image and an $I(U)$ curve was recorded (Figure 3).

Figure 3 shows three exemplary SEM images of Au structures with tip-to-tip spacings of 12.6, 5, and 1 µm (further SEM images please see Supporting Information) as well as the plot of all taken $I(U)$ curves from this series. All curves exhibit a linear behavior within V = ±700 µV before reaching the current compliance (CC). Starting at 12.6 µm, the conductivity improved through the series up to the point where the tips got into direct contact. The respective ohmic resistances were calculated from the slope of each $I(U)$ curve and were plotted versus the tip-to-tip distances displaying a linear dependency converging to the minimum resistance, which could be attributed to the internal resistance of the setup. By subtracting the internal resistance from measured resistances at each position, the resistivity of the individual wires was derived (for a schematically illustration and equation please refer to Figure S7, Supporting Information). All investigated structures gave resistivities within the range of $\rho = 2.2 \times 10^{-6}$ Ωm to 1.4×10^{-7} Ωm. This deviation

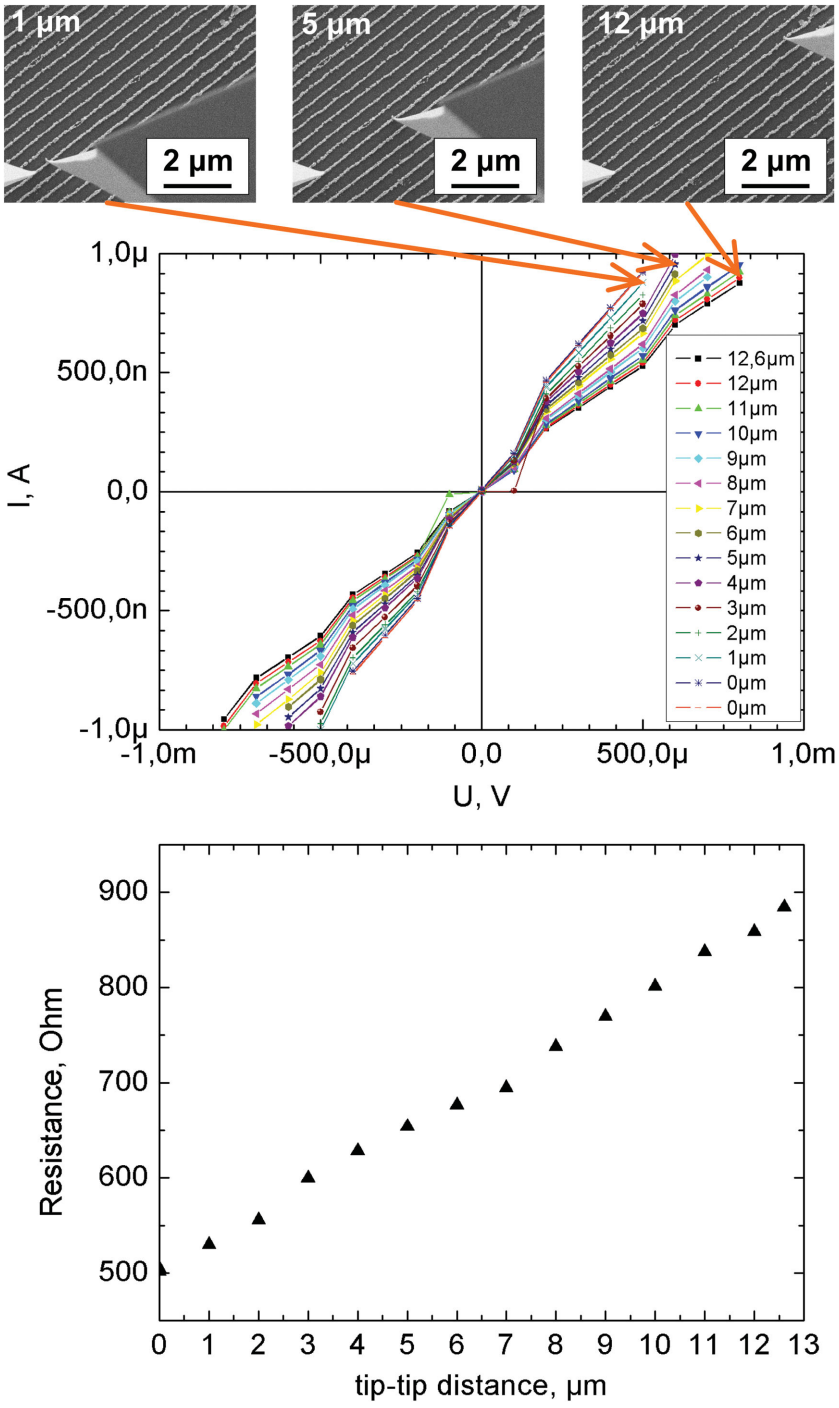

Figure 3. Exemplary SEM images recorded at tip–tip distances of 12.6, 5, and 1 µm (top), as well as the corresponding current–potential plots *I*(*U*) for all distances (center); the thereof resulting ohmic resistance plotted versus the tip–tip distance (bottom).

results from variation in the granular structures itself. Compared to the resistivity of bulk gold (ρ_{bulk}Au = 2.2 × 10^{-8} Ωm), our derived resistivities are only one to two orders in magnitude higher. Similar values have been obtained for polycrystalline nanowires[29–31] and electroless plated structures.[28,32,33]

3. Conclusion

Concluding, we demonstrate a highly flexible, cost-efficient two-step process for the generation of uniform, large array conductive gold nanowire patterns. Essential step of the present work was the successful transfer of the micropattern from the PDMS stamp to the hydrogel. Surface functionalization of both, the silicon substrate as well as the PDMS stamp, enables the large scale transfer of the pattern. Hydrophobic modification lowered the adhesion of the in situ formed polymer at the PDMS surface. The introduction of vinyl groups on the silicon wafer enhanced the covalent binding of the developing polymer. Incorporation of gold(III) ions by coordination, subsequent reduction, and soft template removal via oxygen plasma yields perfectly separated nanowire arrays without loss of geometry. After development of the metal, the generated structures revealed a low resistivity with 3 × 10^{-7} Ωm on average, which is close to the value of bulk gold (2.2 × 10^{-8} Ωm), indicating the production of high quality gold nanowires. The here presented results serve as a proof-of-concept for the generation of 1D gold patterns 200–300 nm in width and approximately 1 µm in distance from wire to wire.

Compared to EBL and other well-established techniques, our approach might have still a higher amount of substeps. Beneficially, it requires however only cheap equipment and materials, which make this pathway attractive. This is the case also due to the immanent transformation of micrometer-sized wrinkles to wires with thicknesses in the nanometer range. Further, the presented proof-of-principle allows easy variation of polymers and thereby incorporating many coordination capabilities,[34,35] finally enabling altered inorganic nanowire composition (e.g., for Ag or Pt nanowires).[36–38] In addition, the approach is not only limited to the linearly wrinkled PDMS template, as shown in this paper. For example, a reusable stamp with more complex features can be generated to produce complex patterns with varying dimensions. This finally envisions

a printing process for entire large-scale nanochips using the presented approach.[39,40]

4. Experimental Section

Preparation of Hydrogel Microstructures: In a 10:1 ratio Sylgard 184 Silicone elastomer Kit (Dow Corning) was homogeneously stirred with curing agent (Dow Corning) and poured into a petri dish. After curing overnight at room temperature, the polymer was heated for 2 h at 80 °C for complete crosslinking. The 3 mm thick PDMS was cut into 10 mm × 13 mm parts which were 1.3-fold stretched with a custom made stretching device. O_2 plasma (480 s, 200 mbar, and 100 W) was used to oxidize the PDMS and generate a thin silica layer. After relaxation of the stretched polymer substrate, the bilayer surface wrinkled up to a sinoidal pattern. For the hydrogel-imprinting process, the substrates were functionalized in a desiccator at 1 mbar and room temperature with trichloro(1H,1H,2H,2H-perfluorooctyl)silane, 97% (Sigma-Aldrich) for 2 h.

To ensure a strong binding of the later polymerized hydrogel on the silicon wafer, the surface was functionalized with 3-(trimethoxysilyl)propyl methacrylate, 98% (Sigma-Aldrich), after thoroughly cleaning with toluene, ISO (VWR), and CO_2 Jet system. The surface modification was carried out overnight in a solution of 1 mL 3-(trimethoxysilyl)propyl methacrylate in 12 mL ammonium hydroxide solution 28%–30% (Sigma-Aldrich) and 75 mL ethanol absolute (VWR). Degassed, ultrapure water was used from a Millipore water purification system with a minimum resistivity of 18 MΩ cm^3. A 10 mL aqueous solution consisted of 8.8 mmol N-vinyimidazole, ≥99% (Sigma-Aldrich), and 0.01eq N,N′-methylenbis(acrylamide) (Sigma-Aldrich), and later mixed with 0.1 mmol of the initiator potassium persulfate (PPS), ≥99.0% (Sigma-Aldrich) was enriched with 10 µL N,N,N′,N′ tetramethylethylendiamine, 99% (Sigma-Aldrich), and after transferring them on the modified wafer, the system was pressed with the PDMS substrate, so that the free radical polymerization, performed in nitrogen atmosphere, could take place in the grooves at room temperature overnight.

Fabrication of Gold Nanowires: The incorporation of gold into the hydrogel was achieved by placing the hydrogel structures in a 10×10^{-3} M aqueous solution of tetrachloroauric(III) acid trihydrate, ≥99.9% trace metals basis (Sigma-Aldrich) for 10 min. After washing and drying under vacuum, the structure was treated with O_2 plasma, at (1 h at 200 mbar and 100 W). The plasma-reduced Au was developed by a modified method described by Schaal et al.[30] By mixing 50 µL of 50×10^{-3} M aqueous solution of tetrachloroauric(III) acid trihydrate in ultrapure water with the same amount of 0.6 M solution of potassium thiocyanate (Sigma-Aldrich) the mixture was diluted at pH 5 in 800 mL of 50×10^{-3} M phosphate buffer. After mixing the colorless solution with 25 µL of 0.05×10^{-3} M hydroquinone solution and stirring, the prestructure was incubated in this solution for 30 s and rinsed with ultrapure water. Finally, the substrate was dried in a nitrogen stream.

Characterization: Morphology characterization of the PDMS stamps, the hydrogel micro- and the gold nanostructures was done by scanning force microscope (ICON Dimension, Veeco) in TappingMode, equipped with a pyramid-shaped silicon-nitride tips (OMCL-AC, Olympus, spring-constant: 44.2– 49.9 N m^{-1}).

The metal nanopatterns where visualized with the scanning electron microscope UHR FE-SEM SU 9000 from Hitachi. The software for providing energy-dispersive X-ray spectroscopy at the UHR FE-SEM SU 9000 (Aztec) was developed by Oxford.

Setup for Electrical In Situ Measurements: The experimental setup applied for the electrical in situ measurements is published in detail elsewhere,[41] but the key elements shall be described briefly. The measurements were realized by means of a nanorobotics system (Klocke Nanotechnik, Aachen, Germany, www.nanomotor.de) in a SEM (Zeiss/LEO Supra 35VP). For electrical addressing, the manipulators were equipped with silicon SFM tips (Nanosensors, ATEC-NC, spring constant 20–110 N m^{-1}), which were freshly coated with at least 25 nm Pt/Ir. The measurements were carried out by using a semiconductor parameter analyzer (Agilent 4156C). During the recording of the electrical currents, the electron beam was blanked out by using a beam blanker unit of the built-in lithography system (Raith, Dortmund, Germany). The nanomanipulators are based on three piezo crystal driven motors for each axis (x, y, z) and allow a positioning with sub-nanometer precision.

In order to remove charging effects from the incident primary electrons, the samples and tips were grounded before starting the electrical measurements. The resistance of the setup, including the contributions of plugs, wiring, and metal coating, was determined prior to the measurements of the structures by moving both tips into direct contact (short circuit). From the slope of the linear $I(U)$ curve, the ohmic resistance could be calculated to R_{setup} = 500–600 Ω exhibiting a sufficiently high conductivity. This value is strictly depending from contact area and coating thickness. Therefore, bias resistance is checked for every set of tips. Under simultaneous observation in the SEM, two conducting tips were approached to the surface or structure of interest until the detection of a slight deformation of the cantilever. To protect the tips and structure from high electric fields and joule heating, a CC was applied limiting the current to I = 1 µA.

Supporting Information

Supporting Information is available from the Wiley Online Library or from the author.

Acknowledgements: The authors gratefully acknowledge the Deutsche Forschungsgemeinschaft within SFB 985 "Funktionelle Mikrogele und Mikrogelsysteme" for financial support. This work was also performed in part at the Center for Chemical Polymer Technology CPT, which was supported by the EU and the federal state of North Rhine-Westphalia (Grant No. EFRE 30 00 883 02).

Received: May 17, 2016; Revised: June 17, 2016; Published online: July 8, 2016; DOI: 10.1002/marc.201600287

Keywords: 1D structures; Au nanoarrays; microgel; nanoimprint lithography; thin films

[1] Q. H. Chi, Y. S. Zhao, J. Yao, *J. Mater. Chem.* **2012**, *22*, 4136.
[2] N. Du, H. Zhang, D. Yang, *Nanoscale* **2012**, *4*, 5517.

[3] L. Lu, S. Jun, *Biosens. Bioelectron.* **2012**, *36*, 257.
[4] S. Shikha, S. Sudha, *Biosens. Bioelectron.* **2013**, *50*, 174.
[5] X. Yin, T. P. Vinod, D. Mogiliansky, R. Jelinek, *Adv. Mater. Interfaces* **2015**, *2*, 1400430.
[6] W. Yan, M. L. Thai, R. Dutta, X. Li, W. Xing, R. M. Penner, *ACS Appl. Mater. Interfaces* **2014**, *6*, 5018.
[7] C. Xiang, S.-C. Kung, D. K. Taggart, F. Yang, M. A. Thompson, A. G. Güell, Y. Yang, R. M. Penner, *ACS Nano* **2008**, *2*, 1939.
[8] W.-K. Lee, S. Chen, A. Chilkoti, S. Zauscher, *Small* **2007**, *3*, 249.
[9] H. Jiang, T. P. Vinod, R. Jelnek, *Adv. Mater. Interfaces* **2014**, *1*, 1400187.
[10] S. Kundu, A. Leelavathi, G. Madras, N. Ravishankar, *Langmuir* **2014**, *30*, 12690.
[11] Z. Nie, A. Petukhova, E. Kumacheva, *Nat. Nanotechnol.* **2010**, *5*, 15.
[12] R. K. Joshi, J. J. Schneider, *Chem. Soc. Rev.* **2013**, *50*, 5285.
[13] Q. Xu, R. M. Rioux, G. M. Whitesides, *ACS Nano* **2012**, *1*, 215.
[14] Q. Xu, R. M. Rioux, M. D. Dickey, G. M. Whitesides, *Acc. Chem. Res.* **2008**, *41*, 1566.
[15] N. Bowden, S. Brittian, A. G. Ecvans, J. W. Hutchinson, G. M. Whitesides, *Nature* **1998**, *393*, 146.
[16] D. Qin, Y. Xia, G. M. Whitesides, *Nat. Protoc.* **2010**, *5*, 491.
[17] Q. Zhou, P. T. Kühn, T. Huisman, E. Nieboer, C. v. Zwol, T. G. v. Kooten, P. v. Rijn, *Sci. Rep.* **2015**, *5*, 16240.
[18] N. Bowden, W. T. S. Huck, K. E. Paul, G. M. Whitesides, *Appl. Phys. Lett.* **1999**, *75*, 2557.
[19] S. Hiltl, J. Oltmanns, A. Böker, *Nanoscale* **2012**, *4*, 7338.
[20] D. Breid, A. J. Crosby, *Soft Matter* **2013**, *9*, 3624.
[21] N. Pazos-Pérez, W. Ni, A. Schweikart, R. A. Alvarez-Puebla, A. Fery, L. M. Liz-Marzán, *Chem. Sci.* **2010**, *1*, 174.
[22] S. Hiltl, M.-P. Schürings, A. Balaceanu, V. Mayorga, C. Liedel, A. Pich, A. Böker, *Soft Matter* **2011**, *7*, 8231.
[23] B. L. Rivas, S. A. Pooley, E. D. Pereira, R. Cid, M. Luna, M. A. Jara, K. E. Geckeler, *J. Appl. Polym. Sci.* **2005**, *96*, 222.
[24] O. Mergel, A. P. H. Gelissen, P. Wünnemann, U. Simon, A. Böker, F. A. Plamper, *J. Phys. Chem. C* **2014**, *118*, 1326199.
[25] O. Mergel, P. Wünnemann, U. Simon, A. Böker, F. A. Plamper, *Chem. Mater.* **2015**, *27*, 7306.
[26] A. Morag, V. Ezersky, N. Froumin, D. Mogiliansky, R. Jelinek, *Chem. Commun.* **2013**, *49*, 8552.
[27] O. V. Lebedeva, Y. N. Pozhideav, N. S. Shaglaeva, A. S. Pozdnyakov, S. S. Bochkareva, *Theor. Found. Chem. Eng.* **2010**, *44*, 786.
[28] J. Timper, K. Gutsmiedl, C. Wirges, J. Broda, M. Noyong, J. Mayer, T. Carell, U. Simon, *Angew. Chem. Int. Ed.* **2012**, *51*, 7586.
[29] J. H. Song, Y. Wu, B. Messer, H. Kind, P. Yang, *J. Am. Chem. Soc.* **2001**, *123*, 10397.
[30] S. Y. Xu, J. Xu, M. L. Tian, *Nanotechnology* **2006**, *17*, 1470.
[31] E. J. Menke, M. A. Thompson, C. Xiang, L. C. Yang, R. M. Penner, *Nat. Mater.* **2006**, *5*, 914.
[32] P. A. Schaal, A. Besmehn, E. Maynicke, M. Noyong, B. Beschoten, U. Simon, *Langmuir* **2012**, *28*, 2448.
[33] K. Keren, M. Krueger, R. Gilad, G. Ben-Yoseph, U. Sivan, E. Braun, *Science* **2002**, *297*, 72.
[34] D. Peralta-Dominguez, M. Rodrigues, G. Ramos-Ortiz, J. L. Maldonado, D. Luna-Moreno, M. Ortiz-Gutierrez, V. Barba, *Sens. Actuator, B* **2016**, *225*, 221.
[35] M. Trigo-López, A. Muñoz, S. Ibeas, F. Serna, F. C. García, J. M. García, *Sens. Actuator, B* **2016**, *226*, 118.
[36] D. Paripovic, H.-A. Klok, *ACS Appl. Mater. Interfaces* **2011**, *3*, 910.
[37] D. H. Gold, H. P. Gregor, *J. Phys. Chem.* **1960**, *64*, 1461.
[38] S. Ghosh, E. Ostrowski, R. Yang, D. Debnath, P. X.-L. Feng, C. A. Zorman, R. M. Sankaran, *Plasma. Chem. Plasma Process.* **2016**, *36*, 295.
[39] M. Gierling, P. Schneeweiss, G. Visanescu, P. Federsel, M. Häffner, D. P. Kern, T. E. Judd, A. Günther, J. Fortágh, *Nat. Nanotechnol.* **2011**, *6*, 446.
[40] J. F. Fennell, S. F. Liu, J. M Azzarelli, J. G. Weis, S. Rochat, K. Mirica, J. B. Ravnsbæk, T. M. Swager, *Angew. Chem. Int. Ed.* **2016**, *55*, 1266.
[41] M. Noyong, K. Blech, A. Rosenberger, V. Klocke, U. Simon, *Meas. Sci. Technol.* **2007**, *18*, N84.